Technical & Programmatic Annex
April 2004

EarthCARE - Earth Clouds, Aerosols and Radiation Explorer
SPECTRA - Surface Processes and Ecosystem Changes Through Response Analysis
WALES - Water Vapour Lidar Experiment in Space
ACE+ - Atmosphere and Climate Explorer
EGPM - European Contribution to Global Precipitation Measurement
Swarm - The Earth's Magnetic Field and Environment Explorers

European Space Agency
Agence spatiale européenne

REPORTS FOR MISSION SELECTION
THE SIX CANDIDATE EARTH EXPLORER MISSIONS

Annex to ESA SP-1279(5)
April 2004

REPORTS FOR MISSION SELECTION
THE SIX CANDIDATE EARTH EXPLORER MISSIONS

EGPM – European Global Precipitation Measurement Technical and Programmatic Annex

European Space Agency
Agence Spatiale Européenne

Contents

1 Introduction

This document provides the technical description of the EGPM mission candidate, as derived from the preparatory activities at phase A level, for implementation as an Earth Explorer in the frame of ESA's Living Planet Programme. It shows how feasible implementation concepts can respond to the scientific mission requirements defined in the Science Report. To this end, the expected system performance will also be described. A summary assessment of the programmatic framework is also provided. The system description is mainly based on the results of work performed during two parallel phase A system studies by two industrial consortia. It is not possible to describe in this report all technical concepts, but where necessary, two concepts are described in order to present significantly different approaches to meeting the mission observation requirements. The description of particular concepts does not indicate special preferences. After an overview of the mission architecture and the proposed orbit (in Chapters 2 and 3) the space segment will be described in detail (Chapter 4), followed by the ground segment and operations concept (Chapters 5 and 6). Following an overview of the data products (Chapter 7), the overall performance is described (Chapter 8). An alternative version without precipitation radar follows (Chapter 9). The report concludes with programmatic considerations (Chapter 10).

2 Mission Architecture Overview

EGPM has its own mission objectives and is also a part of the overall GPM (Global Precipitation Measurement) initiative, which is briefly recalled in the following section.

2.1 GPM Architecture

The aim of GPM is to improve the quantification of the space-time variability of precipitation. The goal is to provide a good quality synoptic view over the complete Earth every 3 hours.

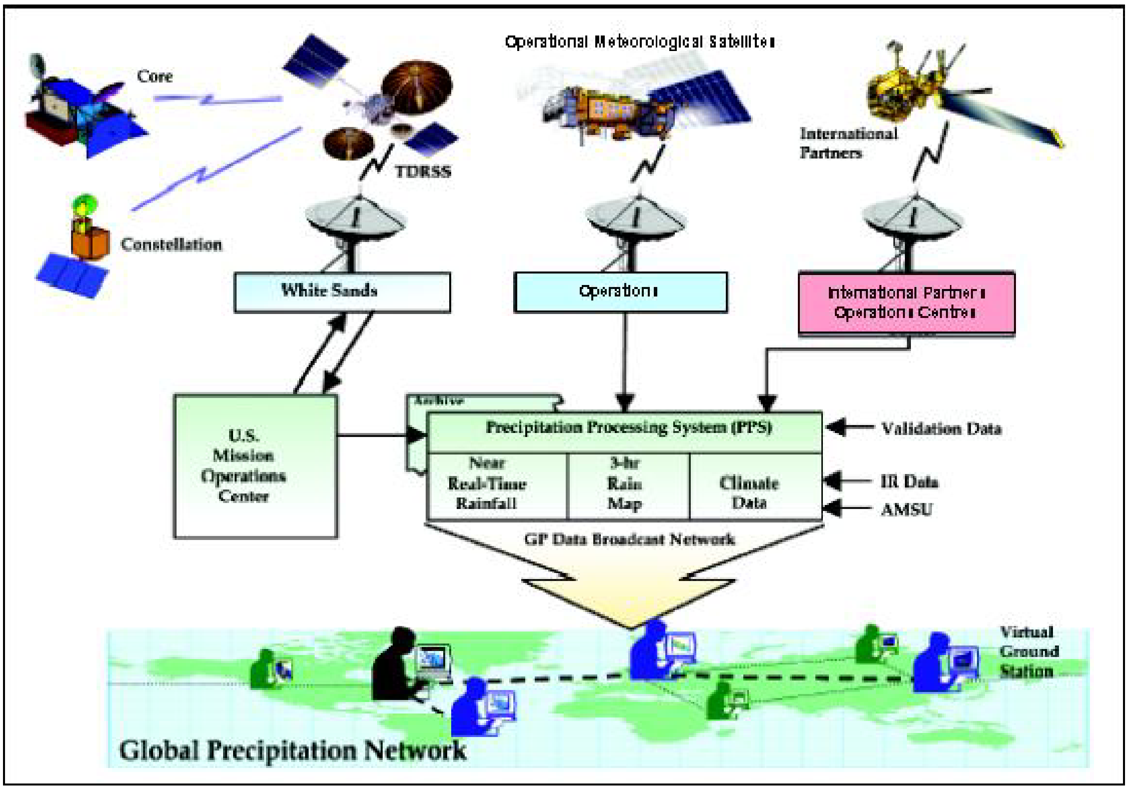

Figure 2.1: *GPM Architecture (as per NASA GPM White Paper July 2002)*

The GPM includes: a NASA-JAXA 'Core' satellite, carrying a microwave radiometer and a dual frequency precipitation radar; passive microwave radiometers flying on operational meteorological satellites and some dedicated satellites to be provided by international partners and NASA. It includes also a central Precipitation Processing System (PPS) and a ground calibration network. The PPS will use the information provided by all the GPM satellites, as well as that provided by microwave and infrared sounders flying in polar orbiting operational meteorological satellites.

The 'Core' satellite will fly in an orbit at 65^{o} inclination and 400 km altitude. The passive microwave radiometers will fly in sun-synchronous orbits. NASA is planning to fly a satellite with a supplementary radiometer at 635 km altitude while the international partners will choose their own orbits.

2.2 EGPM Architecture

The principal elements of the mission are:

- A satellite with two instruments, namely a conically-scanning microwave radiometer and a precipitation radar, flying in a sun-synchronous orbit;
- A dedicated launcher;
- A ground segment, including the Command and Data Acquisition Element (CDAE), the Mission Operations and Satellite Control Element (MSCE) and the Processing and Archiving Element (PAE). The ground segment includes also the data links with the users, with the overall GPM PPS and with any other related external entity.

EGPM will be able to provide data to three types of users:

- Climate scientists, with no special time constraints in the delivery of data
- Near-real-time users, e.g. numerical weather prediction (NWP) users, that need the data within 3 hours of observation
- Real-time 'now-casting' users for monitoring and forecasting of Mediterranean flash floods, requiring the data within 15 minutes of observation. This capability could be extended to other areas.

A simplified EGPM architecture identical to the baseline, with the microwave radiometer but without the radar, has also been considered. It will need to make use of the limited cross-overs with the GPM Core satellite for calibration. It is described in Chapter 9.

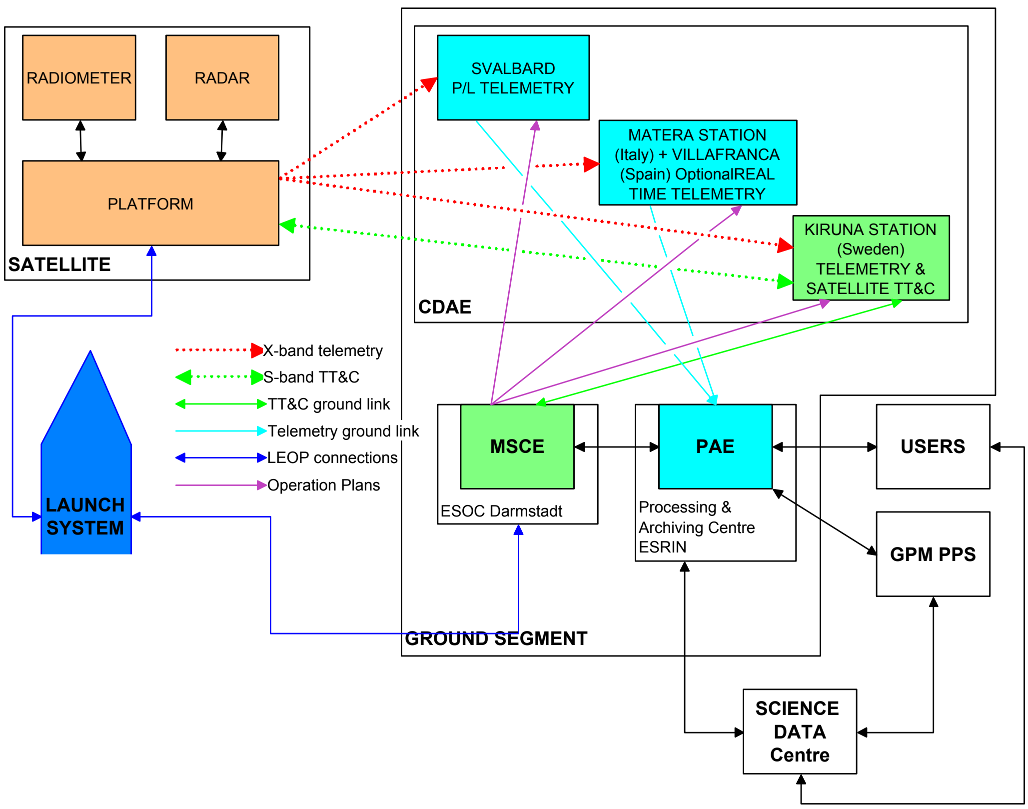

Figure 2.2: EGPM Mission Architecture

3 Orbit

As GPM is a confederation of new and existing assets not originally conceived for the purpose of GPM, it is not possible to derive a sharply defined set of coverage-driven orbit requirements for EGPM. A binning parameter has been used as figure of merit for GPM and EGPM. The day is split into 8 three-hour bins for each of the 500 by 500 km- pixels in which the globe is divided. The more bins covered the better. EGPM is also designed to pay special attention to the coverage of Europe, the Mediterranean area and Canada.

The EGPM mission requirements can be fulfilled with a sun-synchronous orbit. The orbit most complementary to the other sun-synchronous GPM elements has a Local Time of the Descending Node (LTDN) at 14:30. This orbit is also adequate for the observation of intense convective events over Europe.

To allow for the reuse of the data exploitation experience acquired with past missions, the conical scanning angle of the radiometer is fixed at 52.8°. This makes the instrument swath a function of the orbit altitude only. Higher orbits are therefore preferred for coverage, but they require larger antenna sizes and higher power consumption. On the other hand, lower orbits require more fuel to compensate the atmospheric drag and the ground contact opportunities are shorter. A range of orbit altitudes between 450 and 675 km has been considered. At 450 km altitude 45 % of the area of the Earth is covered by EGPM in one day. The corresponding value for the higher end of 675 km is 55 %. The cumulative coverage for Europe defined in a six hours rolling window, can be seen in Figure 3.1. The advantage of the higher orbit is small but clear. A narrower orbital altitude range from 500 to 675 km has been found convenient for design.

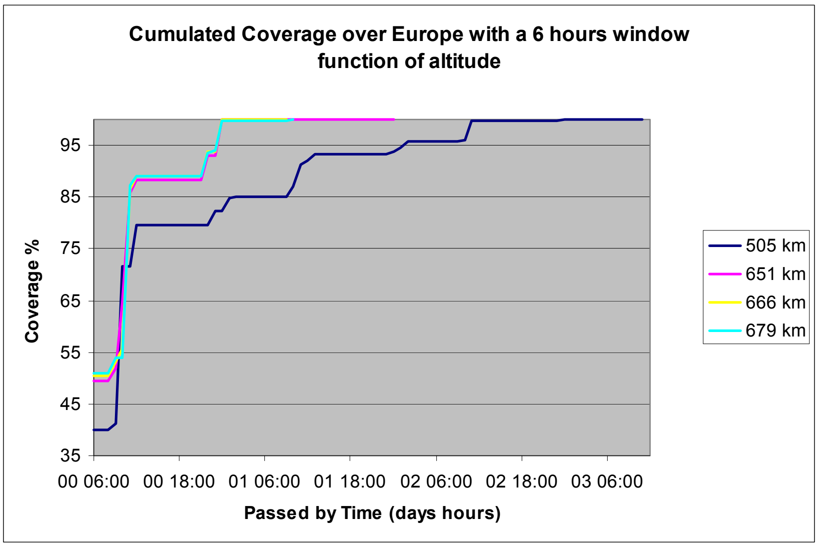

Figure 3.1: *Cumulative coverage over Europe with a 6 hours rolling window*

At 560 km the orbital period is commensurate with the rotation of the Earth. This defines a range of altitudes to be avoided because the orbital pattern will repeat itself every day and many areas will be covered very infrequently as shown in Figure 3.2.

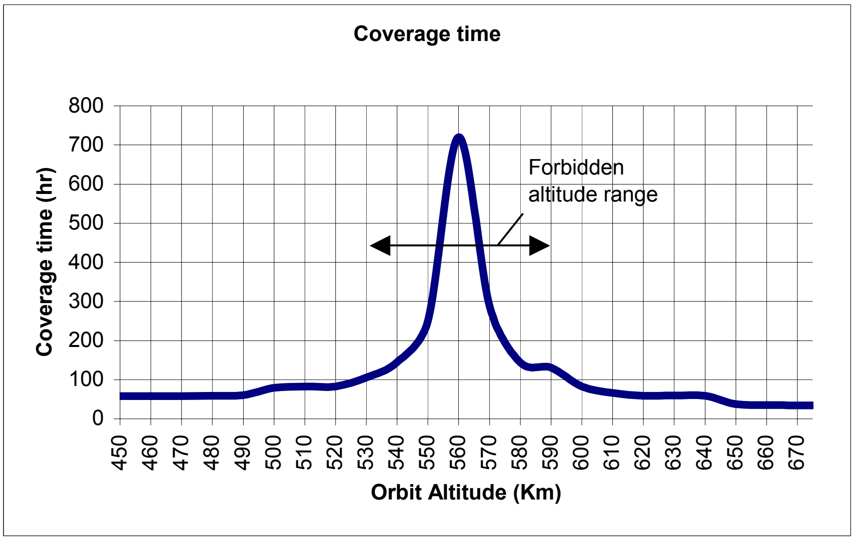

Figure 3.2: *Time for full Earth coverage as a function of the altitude*

An orbit at 666 km would provide full daily coverage over Mediterranean latitudes. The phase A work led to prefer orbits in the 500-520 km altitude range.

4 Space Segment

The EGPM space segment consists of a satellite carrying a conically scanning multi-channel microwave radiometer, section 4.1, with ram and wake viewing capability and a three beam close-to-nadir pointing radar, section 4.2. The two instruments are designed so that the centre reference pixel of the fore view of the radiometer is co-located with the radar footprints. The overlap of the two instruments defined by their -3 dB beam widths is more than 95% along the nadir path. The time difference between the observations of the two instruments is about one minute. The observing geometry is shown in Figure 4.1 and the ground sampling pattern in Figure 4.2.

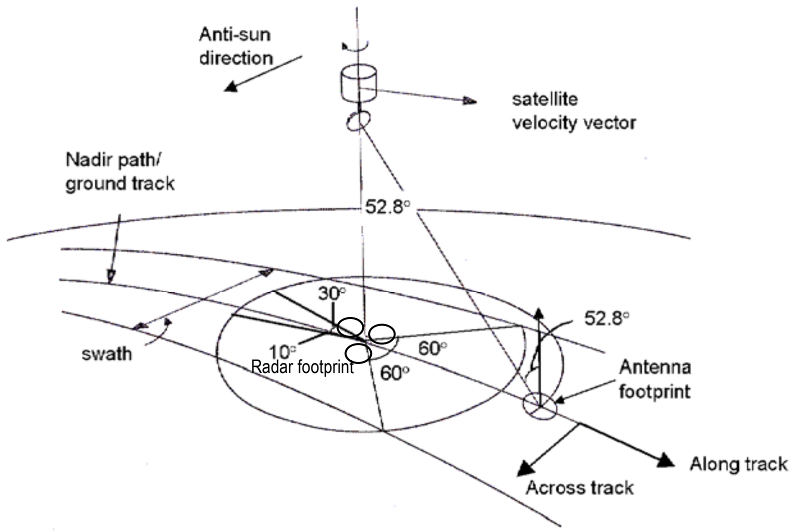

Figure 4.1: *Schematic of the EGPM observing geometry. The conical scanning radiometer track is indicated. The 3 radar beams are represented by the nadir pointing line from the satellite*

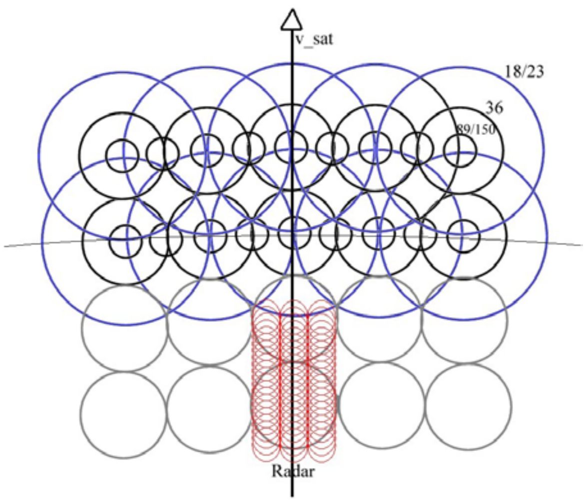

Figure 4.2: *Sampling pattern of the EGPM sensors. The numbers next to the circle indicate the radiometer channel frequency. The small red circles are the radar footprints. The 3 radar beams match the radiometer 36.5 GHz footprint over the sub-satellite track*

4.1 Microwave Radiometer

4.1.1 Instrument Objectives and Requirements

The microwave radiometer measures atmospheric brightness temperature at frequencies between 18.7 and 150 GHz. The channel set consists of:

- Imaging channels, which are the classical window and water-vapor channels
- Profiling channels, which are placed around two strong oxygen emission lines.

Centre Frequency (GHz)	18.7	23.8	36.5	89.0	150.0	50.0 53.0 54.0 55.0	118.75±1.0 118.75±1.5 118.75±2.0 118.75±4.0
Bandwidth (MHz)	200	400	1000	6000	3000	500	1000
Centre frequency stability (MHz)	20	20	50	100	100	50	100
Polarisation	H+V	V	H+V	H+V	H+V	H or V	H or V
Footprint (km × km)	26×26	26×26	13.4×13.4	5.5×5.5	5.5 × 5.5	13.4×13.4	13.4×13.4
NEΔT (K)	0.5	0.6	0.7	1	1	0.5	1
Accuracy (K)	1.5	1.5	1.5	1.5	1.5	1.5	1.5
Differential Accuracy (K)	0.5	0.5	0.5	0.5	0.5	0.5	0.5
Number of Channels	2	1	2	4 or 2	4 or 2	4	4

***Table 4.1:** Microwave radiometer channels and requirements. (NEΔT: Noise equivalent temperature sensitivity)*

4.1.2 Overall architecture

Figure 4.3 shows the two proposed configuration concepts. The instrument consists of a fixed part attached to the platform and a rotating part providing the conical scan capability. A rotary joint through which power command and data lines are provided connects both parts. The instrument interfaces with the satellite data handling by means of a remote terminal unit located in the rotary part. The feeds and the receivers are also contained in the rotating part. The architecture of the receiver can be seen in Figure 4.4. The calibration unit consisting of a hot calibration target and a mirror to reflect cold space into the receivers is mounted on top of the fixed part of the scan mechanism. The scan rate of approximately 31 rpm, the instantaneous field of view and the integration time of the reference channel (36.5 GHz) are adjusted to the satellite speed, the incidence angle of 52.8 deg and the swath in a way to provide full ground coverage. Compensation of the momentum generated by the large rotating mass is performed by the attitude control of the platform.

The instrument ram and wake views are limited by the need to provide space for the hot and cold calibration and to avoid interference with the radar, the solar array and the satellite body. For the proposed designs, the ram swath angle with respect to the sub-satellite track, is = ±60˚ and the wake is +10˚ ÷-30˚. The wake view asymmetry is due to the different size of the calibration targets.

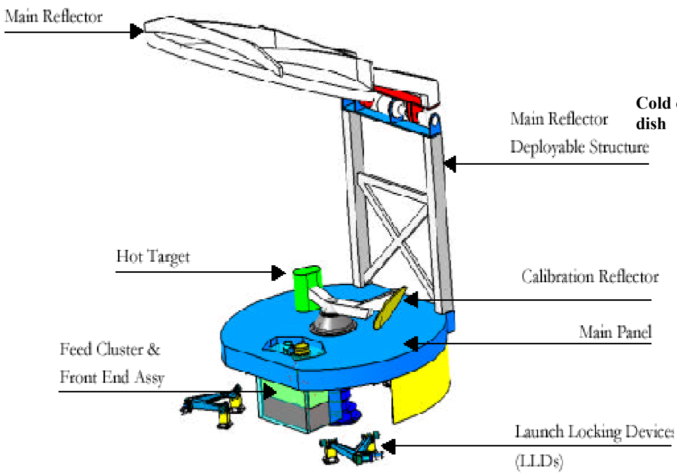

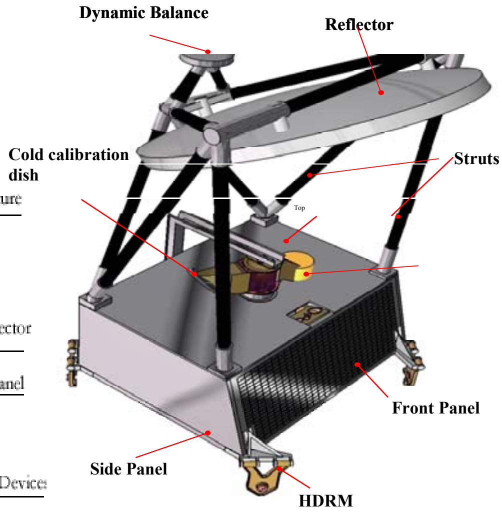

Figure 4.3: *Microwave radiometer configuration concepts: A (left), B (right)*

4.1.3 Radiometer Mechanical Configuration

In concept A, Figure 4.3, the main carbon fibre reflector is stowed during launch and deployed in orbit. The scan mechanism is mounted around a column that is attached to the platform top panel. The power and data transfer is realised through a number of conventional slip-rings based on developments done in the MIMR programme. In concept B, the reflector is mounted on rigid struts. The L-shaped U-profile above the top panel supports the tip of the rotary mechanism, which is also supported at the bottom to the platform top panel. Power transfer is realised through the ball bearings of the rotary joint and data lines via contact-less capacitive coupling. For some start up lines, conventional slip rings will also be implemented. The reflector diameter will be around 1.2 m for the 520 km of altitude. The radiometer is locked to the satellite by 3 or 4 locking devices that unload the bearings of the rotary joint during launch. Structural analysis has demonstrated the adequacy of both design concepts.

To improve satellite pointing, the rotary part of the satellite shall be carefully balanced. Allocations for angular misalignment and for static and dynamic unbalance have been provided. The allocated values are compatible with reasonable manufacturing and assembly tolerances, and with the stiffness and dimensional stability of the proposed design. The contribution of the radiometer unbalance to pointing errors is included in the table of section 4.4.3. The thermal control design concept includes radiators and heaters. Calculations have demonstrated the suitability of the design.

4.1.4 Front End

The microwave radiometer has 19 or 21 channels in 7 frequency bands as listed in Table 4.1. The achieved performance is provided in chapter 8. The non-sounding channels can be seen in the upper part of Figure 4.4. In one of the proposed concepts, direct detection is used for the four lower frequencies while heterodyne detection is used for the highest frequency, at 150 GHz. The profiling channels are depicted in the lower part of the figure. Direct detection is used for the 50 – 55 GHz set while heterodyne detection is used for the set of channels in the 118 GHz frequency range.

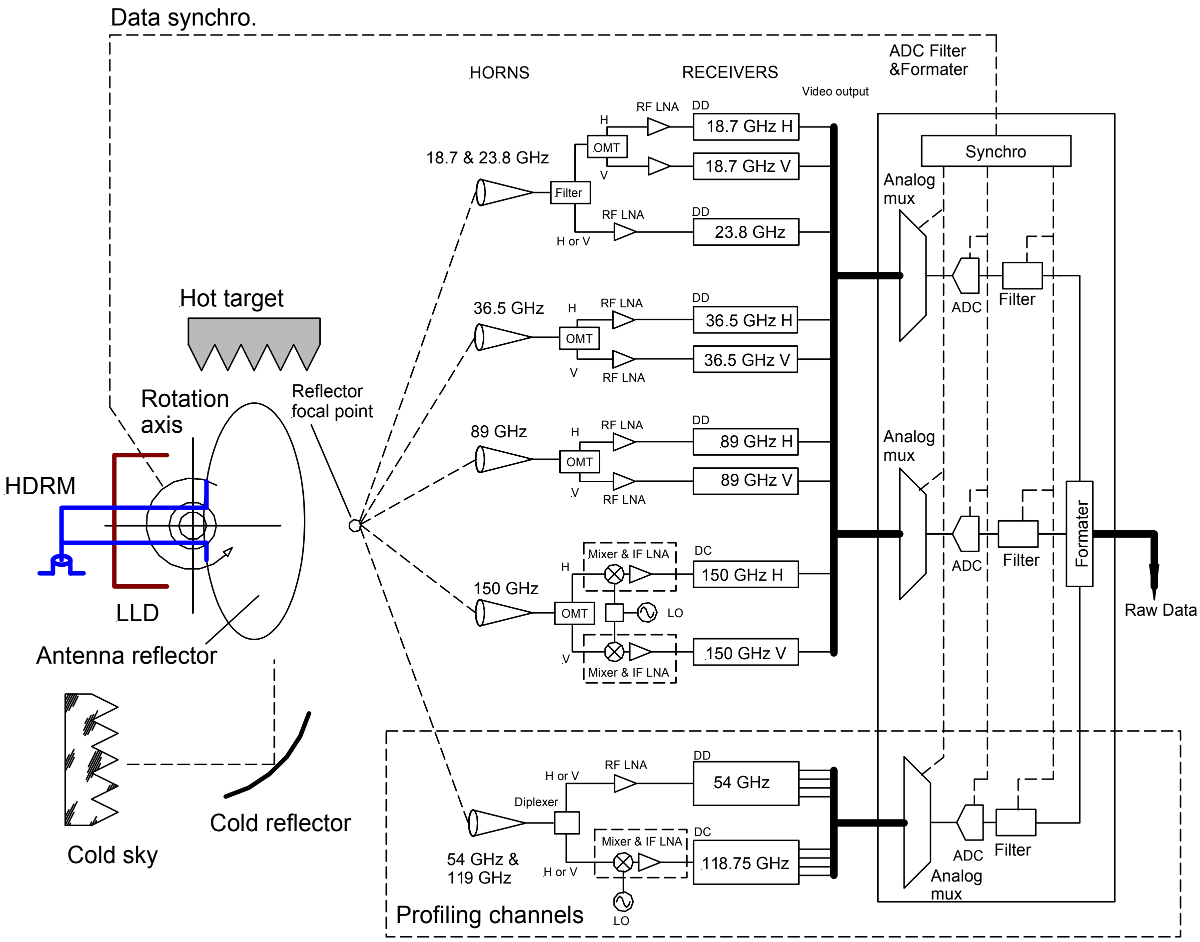

Figure 4.4: *Radiometer Receiver Architecture*

Figure 4.5 shows the feed cluster arrangement for one of the proposed instrument concepts. Dual frequency feed horns are used for the channels at 18/23 GHz and 54/118 GHz. The front-end design of concept A, is strongly based on previous experience and on on-going technology development. Details on development status of front-end technologies are provided in chapter 10.

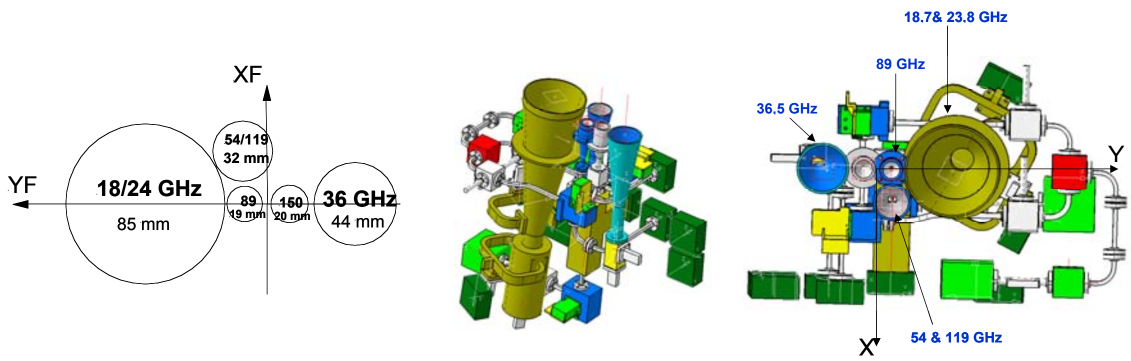

Figure 4.5: *Feed cluster geometry and configuration of one of the concepts*

4.1.5 Back end and Electronics

This unit provides data acquisition, processing functions and scan mechanism control. With respect to processing, the design drivers are the performance of the analog to digital conversion (ADC), and the multiplexing of the channel acquisition functions. Analysis suggests that 3 ADC's with 12 bits resolution can provide the needed accuracy. The other main function of the electronics is the control of the scanning mechanism, which is implemented, with two modes of control. The speed control is the nominal operational mode. The position control is used when the mechanism has to be stopped in a safe position. The control loop will use a 21 bits position encoder to provide the required pointing and position accuracy.

4.1.6 Instrument Budgets

Depending on the concept, the radiometer mass will be between 95 and 135 kg. It will consume between 95 and 112 W and produce data at 62 kb/s.

4.2 Precipitation Radar

4.2.1 Instrument Objective and Requirements

The precipitation radar is optimised for the observation of light and solid precipitation. It provides continuous calibration for the microwave radiometer. It operates at 35 GHz by sending pulses which are backscattered by solid and liquid precipitation. The measurement of the backscattered radiation provides a profile of the precipitation along the microwave radiation path. The performance requirements on the precipitation radar expressed in engineering units, are derived from the observation requirements, expressed in precipitation rates, using empirical expressions. The requirements are summarized in table 4.2 and shall be fulfilled for an integration area of 20×20 km.

The range (vertical) resolution of the radar shall be better than 200 m. The vertical observation range is from –7 (for mirror image measurement) to + 15 km. The footprint resolution is 4.3 km per beam. It shall be recalled that the three 4.3 km beams of the radar combine to fill a single footprint of the radiometer 36.5 GHz channel as indicated in Figures 4.1 and 4.2.

Parameter	Requirement			
	Liquid		Solid (*)	
	Threshold	Goal	Threshold	Goal
DYNAMIC RANGE (MM/H)	0.1 to 50	0.1 to 50	0.1 to 20 (**)	0.1 to 20 (**)
True reflectivity range (dBZ) (***)	12.2 to 45	12.2 to 45	5.7 to 51.7	5.7 to 51.7
PRECIPITATION RATE ACCURACY (%)				
Precipitation rate ≤ 1 mm/h	100 (≤ 25.4 dBZ)	50 (≤ 25.4 dBZ)	50% Hit Rate / 50% False Alarm Rate	100 (≤ 25.7 dBZ)
1 < precipitation rate ≤ 10 mm/h	50 (≤ 38 dBZ)	25 (≤ 38 dBZ)		50 (≤ 45.7 dBZ)
Precipitation rate > 10 mm/h	25 (> 38 dBZ)	10 (> 38 dBZ)		25 (> 45.7 dBZ)
	(*) This also includes e.g. hail (**) This is the liquid water equivalent (***) The measurement of high precipitation rates (≥ 15mm/h) shall not drive the radar sensitivity			

Table 4.2: *Radar Sensitivity & Accuracy Requirements*

4.2.2 Overall Architecture

In the proposed concepts, the radar is located on the anti-sun side of the spacecraft as shown in Figure 4.6. This facilitates heat rejection and avoids interference with the microwave radiometer. The antenna is stowed against the outer side of the wall and it is deployed after launch by a spring driven deployment mechanism. The RF unit with the switching matrix, the Klystron and the electronic power conditioning (EPC) are located on the inner side of the wall. Also the digital electronics is accommodated on this panel. The beams are generated by three Ka-band conical horns that are also fixed to that wall.

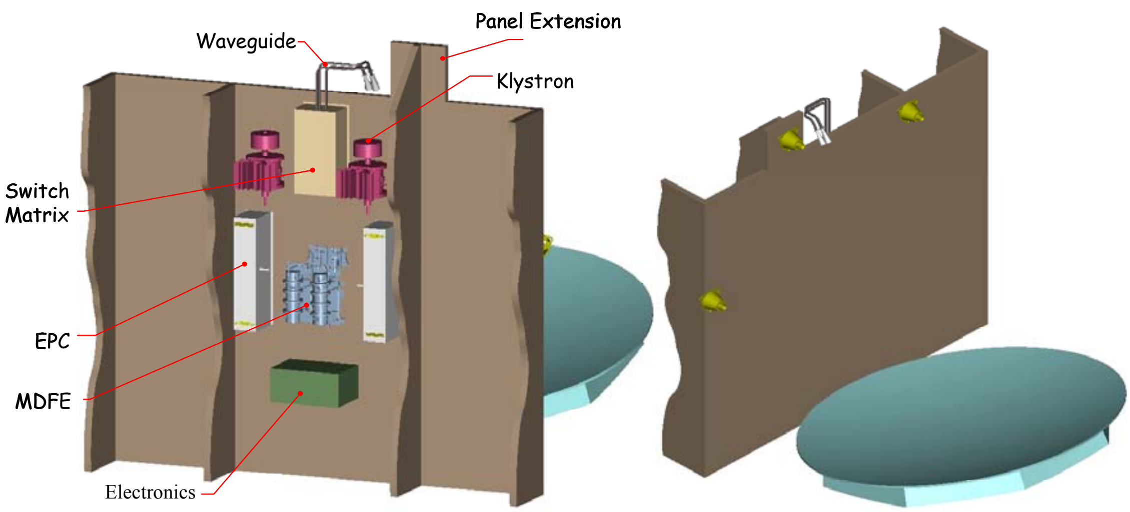

Figure 4.6: *Radar electronics assembly on the backside of the anti-sun panel showing redundancy (left), and the antenna assembly (right)*

4.2.3 Observation geometry

The radar observation geometry has been chosen so as to be able to co-register with the observations of the 36.5 GHz channel of the microwave radiometer, as shown in figure 4.2, and to resolve precipitation inhomogeneity within this radiometer reference footprint (36.5 GHz/ 13 km) along the sub-satellite path. The radar consists of 3 beams (consecutively fired), with footprints located in the tips of a equilateral triangle and forming a continuous swath centred about the sub-satellite track.

4.2.4 Instrument concept

The radar is composed by three main subsystems as shown in Figure 4.7:

- Antenna subsystem
- RF subsystem
- Digital subsystem.

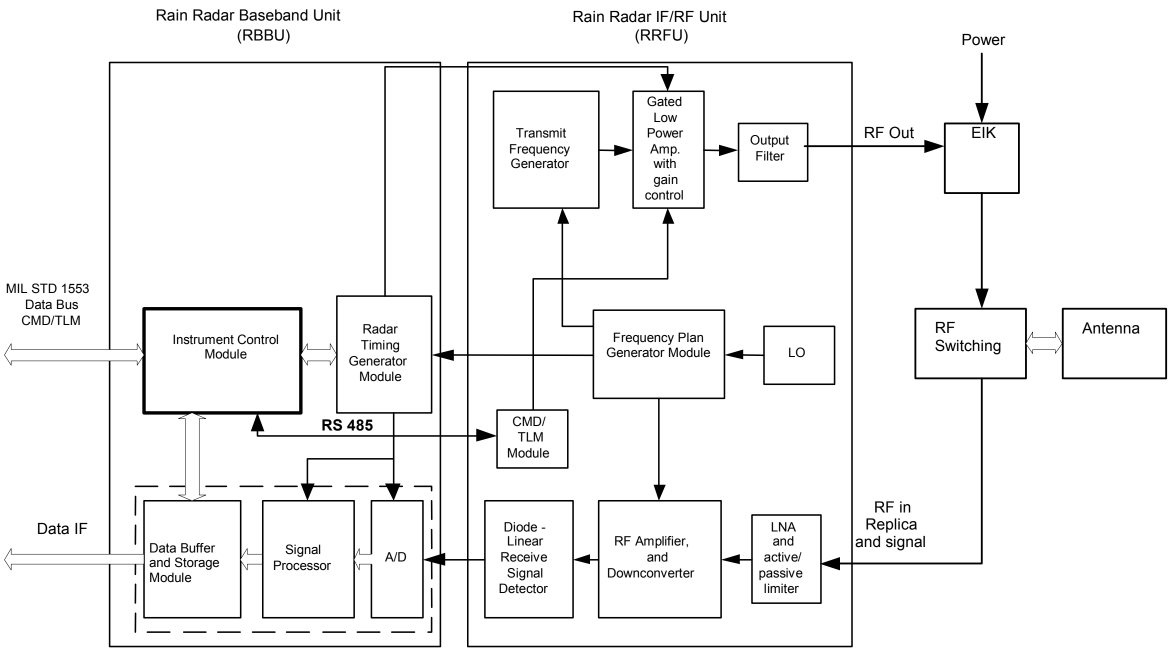

Figure 4.7: *Rain Radar Overall Block Diagram*

The radar antenna is mounted on the anti-sun face of the spacecraft, and its position has been selected in order to avoid the obstruction of the field of view of the microwave radiometer. At 510 km orbit altitude, the carbon fibre reflector antenna can either have a circular aperture with 1.3 m diameter, or have a square aperture (length 1.36 m) in order to provide additional shielding against RF leakage to the radiometer instrument.

The RF subsystem includes the switching network, the power section and the electronic unit. The basic design choice is between long and short pulse radar implementations. The trade-off affects the transmitter power and the transmit / receive signal processing. The short pulse implementation requires a high power amplifier, such as a Travelling Wave Tube Amplifier (TWTA) or an Extended Interaction Klystron (EIK). The long modulated pulse concept requires a digital waveform generator. Subsequently the digitally coded transmit pulse must be converted to an analogue signal at the radar transmit frequency and amplified by low power (approx. 2W) Solid State Power Amplifier (SSPA). This option requires matched pulse compression of the received signal.

The EGPM radar baseline is based on an Extended Interaction Klystron (EIK) derived from the space-qualified CloudSat tube operating at 94 GHz and the development for EarthCARE. The baseline pulse length is 1.67 μs. The pulse repetition frequency is 2767 Hz and the peak power is 1500 W. The transmission and receive chains are significantly simplified adopting this strategy (i.e. no coding of the transmit pulse and no compression of the received signal).

In order for the radar to avoid single point failures all radar electronics, high power amplifier and antenna switch drive electronics are fully redundant.

The RF electronic unit (RRFU in Figure 4.7) is mainly composed by:

- Transmit frequency generation block, that together with the gated low power amplifier provides the 35.505 GHz signal with approximately 50 mW output drive power for the high power amplifier, i.e. the EIK;
- Receiver block composed of a limiter, the low noise amplifier (LNA) and two-stage mixer (down converters) and linear diode detectors that provide the signal to the ADC;
- Frequency generation block which generates the signals for the transmit and receive sections from the low frequency local oscillator (LO);
- Command and Telemetry Module that receives commands through a RS485 connection for controlling the gain of the low power transmit amplifier.

The digital electronics unit (RBBU in Figure 4.7) is in charge of:

- Conversion to digital signals, on board integration (1 km) and storage of the received and calibration data;
- Radar timing;
- Radar monitoring and control.

The radar interfaces via the MIL-1553 bus with the platform data handling.

4.2.5 Instrument Budgets

Depending on the concept, the radar mass will be between 45 and 55 kg. It will consume between 65 and 85 W and it will produce data at 45 kb/s.

4.3 Platform

All the elements of the EGPM platform are well within the state-of-the-art and can be based on proven designs and equipment.

4.3.1 AOCS

As derived from the overall pointing and geo-location budgets, the Attitude and Orbit Control Subsystem (AOCS) has to ensure ±2.4 mrad for the pointing accuracy and 1.4 mrad for pointing knowledge. A conventional three-axis stabilized satellite is the obvious design choice. The AOCS uses reaction wheels as the main attitude control actuators and star-tracker and gyros as sensors. Magneto-torquers are used for wheel momentum unloading. This design provides ±1.41 mrad pointing accuracy and 0.3 mrad for pointing knowledge. The magneto-torquers are also used for initial angular momentum dumping and for safe mode operation. Sun sensors and magnetometers are used as attitude measuring devices for initial acquisition and safe mode operation.

The EGPM satellite carries a large conically scanning radiometer. Unless compensated for, the radiometer angular momentum, of up to 60 Nms, will introduce an undesired gyroscopic effect and make the attitude control of the satellite impossible. Momentum compensation can be provided either by a dedicated wheel with rotation axis parallel to the axis of the radiometer, or by adequate selection of the AOCS wheel size and of the geometric arrangement of the wheels. Both solutions have been studied. In the first case, the dedicated wheel must have a capacity of 80 Nms to compensate the radiometer. In the second case, four wheels of 40 Nms capacity in a flattened pyramid configurations are needed.

The radiometer introduces unbalances due to the asymmetry of its inertia matrix, and these cannot be compensated by the AOCS. Other factors also generate alignment errors between the AOCS reference and the instrument reference frames. All these effects have been accounted for and the resulting pointing errors are compatible with the mission needs, as discussed in detail in section 4.3.3.

4.3.2 Power

The proposed concepts are based on the use of a deployable solar array with triple-junction GaAs cells and Li-Ion batteries with capacity in the range 50 to 84 Ah. The power bus is unregulated with a nominal voltage of 28 V. The solar array can be fixed or rotating. A fixed solar array requires a relatively large area of 7.5 m^2 but can be canted to minimize atmospheric drag. The canting angle is of 159° with respect to the zenith. To improve efficiency, it is possible to rotate the solar array around a longitudinal axis. This improves the efficiency with respect to a fixed solar array and allows for the reduction of the array size to 5 m^2.

4.3.3 Avionics

A proposed functional architecture based on previous Earth Explorers can be seen in Figure 4.8. The concept uses two standard MIL-1553 buses, one for the instruments and one for the platform, and a dedicated line from the mass memory unit to the X band telemetry. An ERC-32 processor is used to control the satellite and the instruments. The on-board computer also manages the redundancy in the satellite. The mass memory stores the instrument data, housekeeping and ancilliary data. The requirements ask for storage of one orbit of instrument data and 3 days of houskeeping data. This corresponds to 900 Mb and to provide a margin, a memory of 3 Gbits is foreseen.

4.3.4 Communications

The telecommand and telemetry communication subsystem is based on redundant S-band transponders, ensuring a standard uplink rate of at least 4 kb/s and a downlink rate of 64 kb/s. Omni-directional antennas ensure the coverage for any satellite attitude.

The payload data is downlinked via a redundant X-band transmitter operating with QPSK modulation at 10 Mb/s. The link margins are adequate: 10-15 dB for the S band and 8 dB for the X band link.

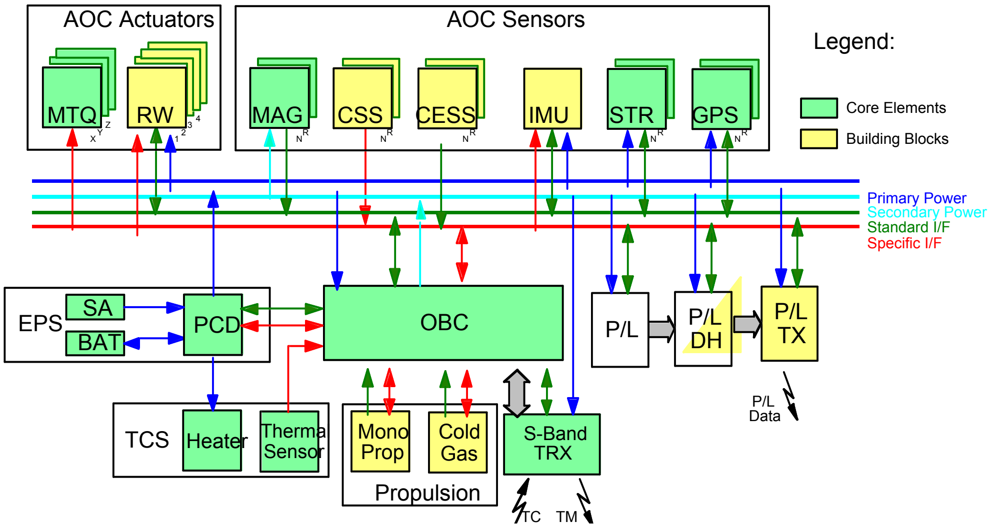

Figure 4.8: *Avionics Architecture*

4.3.5 Propulsion

The propulsion elements are needed to maintain the orbit of the satellite. The main design driver is the compensation of the aerodynamic drag. The concepts proposed use blow-down hydrazine monopropellant systems. The tank volume will depend on the orbit altitude and the drag coefficient of the satellite. For an orbital altitude in the 500-520 km range, the amount of fuel is around 50 kg. Three quarters of the fuel are needed for orbit maintenance and the rest for initial errors correction.

4.3.6 Structure and Thermal Control

The structure and thermal control are quite conventional. The structure can be based on shear panels, on a reticular frame, or on an internal cylinder. The optimal choice will depend on the industrial heritage, taking into account the specific need to accommodate the hydrazine tank. The thermal control elements include heaters and radiators located in the different sides of the platform and in the radiometer. Finite element mechanical and thermal analyses allowed verifying the suitability of the proposed structure and thermal control for the mission. The thermal environment and the radiometer mass property unbalance produce pointing errors. A preliminary analysis of the deformations has been performed and the results have been considered in the pointing budget of chapter 4.4.3.

The structure and thermal control of the satellite are compatible with the overall pointing requirements. An allocation of 0.5 mrad has been provided for structural and thermal deformations. Thermo-elastic analysis results demonstrate the adequacy of the design to fulfil this allocation.

4.4 Satellite

4.4.1 Configuration

The satellite configuration is driven by the need for:

- Providing the radiometer with clear fields of view in the velocity and anti-velocity directions
- Separating as much as possible the radiometer and the radar to ensure the challenging electromagnetic compatibility between them
- Minimizing transversal area to reduce the atmospheric drag

In the proposed concepts, the satellite body has cubic shape with the solar array in the sun side, the radar in the anti-sun side, the interface with the launcher in the nadir side and the radiometer in the zenith face. This provides the clearance in the velocity and anti-velocity directions for the radiometer fore and aft views. The ram view in both cases is ± 60°. The wake view is limited due to the needs to avoid interferences and to accommodate the radiometer calibration targets. In both cases, deployable booms are needed to provide the required X and S band antennas fields of view.

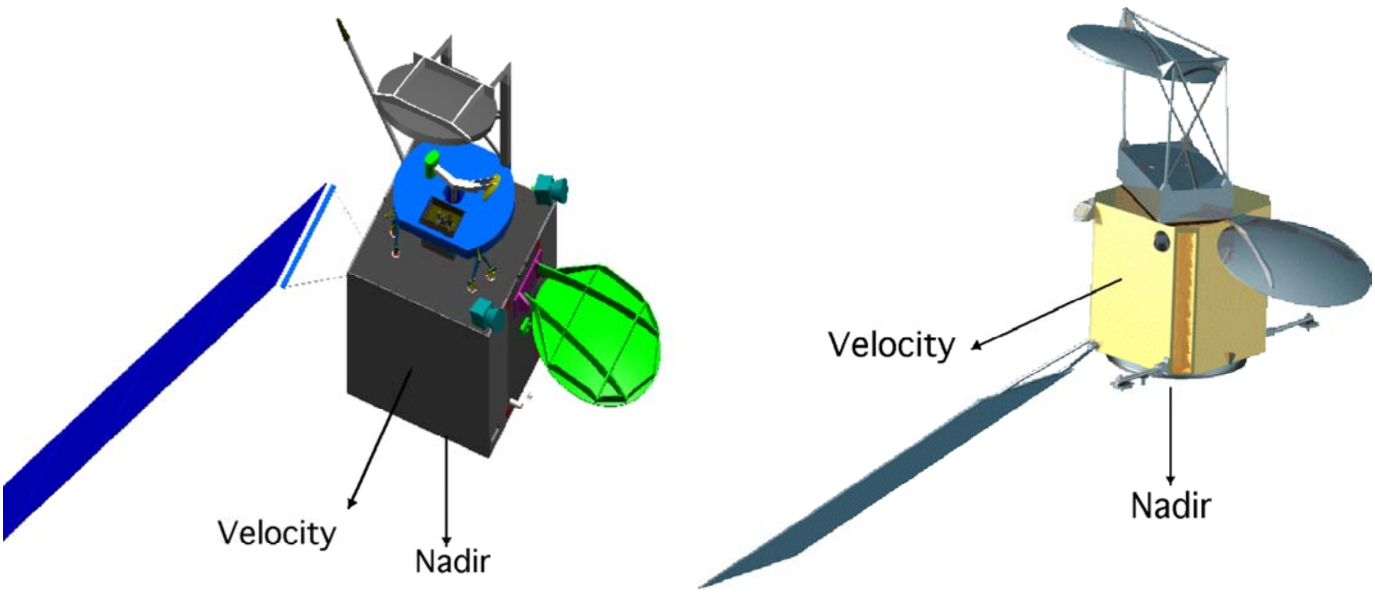

***Figure 4.9:** Two EGPM satellite configuration concepts*

4.4.2 Electro Magnetic Compatibility

EGPM includes a very sensitive radiometer and several powerful transmitters. Transmitter / receiver combinations may experience significant couplings and cause measurement degradation. The baseline EIK based radar transmits a peak of 39 dBm at a frequency of 35.505 GHz. One of the radiometer channels operates at 36.5 GHz ± 500MHz. In terms of the microwave radiometer operation this frequency separation is regarded as critical.

The configuration of the satellite avoids the arrival to the radiometer of radar energy after a single diffraction. Preliminary radio frequency interference analyses show that the coupling attenuation is about –173 dB. Uncertainties and errors reduce that value by 30 dB to -143 dB. The resulting worst-case input power at the radiometer will be –104 dBm, which is well above the radiometer detection threshold of –130 dBm. Given the uncertainties, this demonstrates that the interference problem will need serious effort in the mission implementation phase. The radiometer and radar must incorporate filters at the appropriate frequencies and the radiometer can be blanked during the radar transmission.

4.4.3 Pointing

This is driven by the need of providing 1 km geo-localization and co-registration for the radiometer and radar observations. At the analyzed flying altitude, this induces a requirement of ± 2 mrad. It is also necessary to avoid changes of the radiometer incidence angle which leads to a requirement on pointing accuracy of ± 3.5 mrad.

These values have been used to produce pointing budgets and to allocate admissible errors to the different elements of the satellite. These allocations have been taken into account in the design and analyses has been used to verify the adequacy of the proposed implementation concepts.

	Geo-location	Co-registration	Pointing Error
Radiometer	1.22	1.36	1.36
Radar	N.A.	0.5	N.A.
AOCS	0.3	N.A.	1.41
Structure	0.5	0.5	0.5
Total	1.35	1.54	2
Requirements	2	2	3.5.

Table 4.3: *Pointing error budgets. All values (in mrad) are maximum or 3σ*

4.4.4 Budgets

The satellite power and mass budget for two proposed concepts are as per Table 4.4

Power (W)	Concept A	Concept B	**Mass (kg)**	Concept A	Concept B
Platform	270	370	Platform	390	515
Radiometer	112	95	Radiometer	95	135
Radar	65	85	Radar	45	55
Heaters	20	50	Fuel	35	95
Total + margin	470+50	600+300	TOTAL + MARGIN	530+50	800+80

Table 4.4: *Satellite power and mass budgets*

4.5 Launcher

The mass and volume of the satellite is compatible with several small launchers of the Rockot, Vega and Dneper class. In all cases, there are reasonable volume margins and comfortable mass margins. The requirements envelope for the launchers considered, includes longitudinal stiffness of 35 Hz and transversal stiffness of 15 Hz. The design lateral static acceleration is 1 g and 8.1 g the longitudinal. Compliance with these requirements has been shown by means of structural analysis.

Figure 4.10: *Example of GPM accommodation inside Rockot*

5 Ground Segment

The ground segment will be based on the infrastructure being developed to support the Earth Explorer and other missions. The breakdown of the ground segment into its constituting elements and functions is outlined in Figure 5.3. It consists of three main elements:

- The Command and Data Acquisition Element (CDAE)
- The Mission Operations and Satellite Control Element (MSCE)
- The Processing and Archiving Element (PAE)

These three elements implement the Flight Operations Segment (FOS) and the Payload Data Segment (PDS) functions. The FOS will be developed and operated according to the concept of "family of missions" by means of which several missions share resources and staff for reduction of costs and reutilisation of expertise. Concerning the PDS, the principles and infrastructure developed for the operational, "oxygen" initiative will be reused as well as the infrastructure procured for previous Earth Explorer missions.

The fundamental design drivers are that all EGPM data has to be delivered in less than 3 hours and the Mediterranean data has to be provided in less than 15 minutes. The EGPM ground segment will also exchange data with the GPM PPS. These special requirements result in some novel elements to cope with the needs of the mission.

5.1 Overall Architecture

The near-real-time requirement of 3 hours implies data downlink every orbit. The latitude of Kiruna is not high enough to provide visibility every orbit. With an altitude around 500-520 km, the Svalbard station (Figure 5.1) can communicate with the satellite every orbit, but during several of them, the satellite is only a few degrees above the horizon. Nevertheless, experience indicates that in good weather Svalbard can provide contact with the satellite for elevation as low as 2 degrees over the horizon. This is a marginal situation and the addition of another ground station like Gatineau will provide a more robust ground segment. Kiruna will be the single ground station for satellite commanding and monitoring in S band.

The proposed way to implement the 15 minute Mediterranean nowcasting link is the use of a centralized architecture with Matera (Figure 5.2) receiving all the data acquired over the area of interest in a short downlink, once the area has been covered and near the end of the visibility window. To extend nowcasting coverage to the Atlantic coast of Spain and Portugal, a second ground station, e.g. in Villafranca would need to be included. If needed this nowcasting coverage capability could be expanded to other areas of the Earth but at the expense of complicating the downlink strategy and involving additional ground stations.

Therefore, the architecture, figure 5.3, will include:

- Kiruna for S band up and downlink
- Svalbard for main X band downlink at 10 Mb/s and Gatineau (if needed) to cover the possible blind orbits of Svalbard
- Matera for Mediterranean X band downlink in a short duration downlink at 10 Mb/s

- ESOC for MSCE
- ESRIN for PAE

During Launch and Early Orbit Phase (LEOP), additional suitable ground stations will support operations.

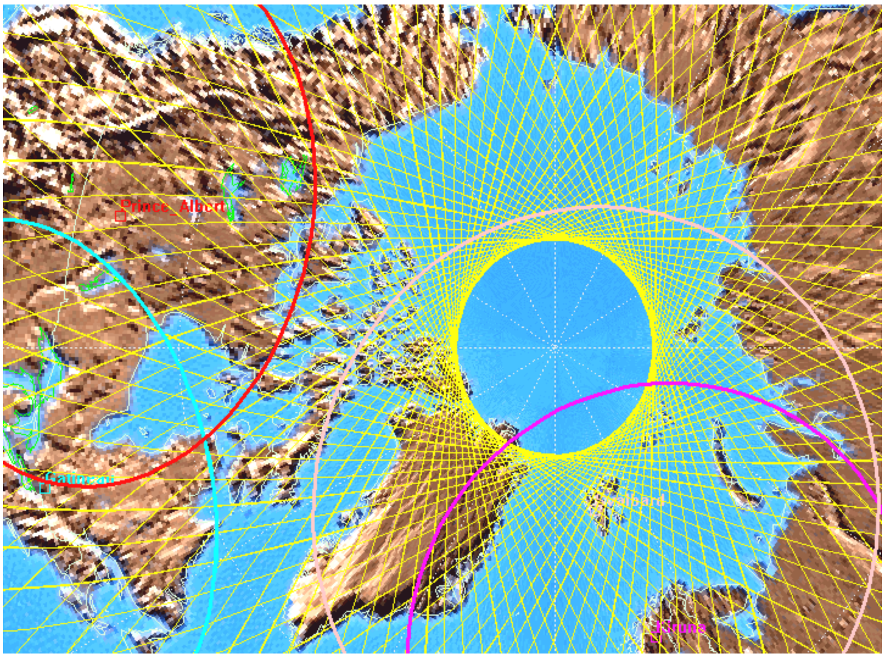

Figure 5.1: *Ground station visibility masks with the satellite at 520 km, Svalbard elevation mask at 2 degrees Kiruna, Gatineau and Prince Albert at 5 degrees*

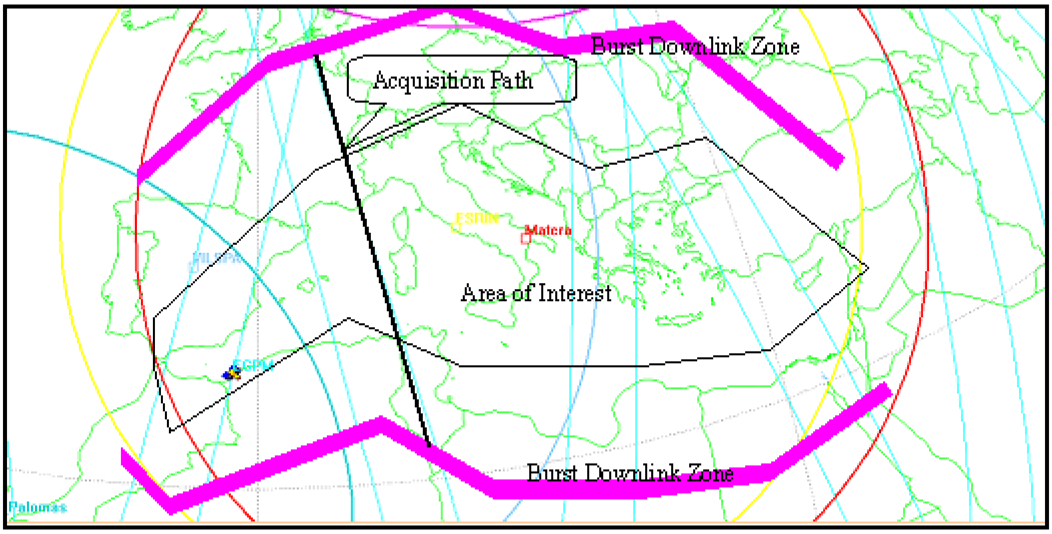

Figure 5.2: *Visibility, area of interest and area of downlink over the Mediterranean*

5.2 Element Functions and Interfaces

The MSCE, located at ESOC, will provide the following main functions:

- Satellite operations planning in connection with the PAE

- Satellite monitoring and control
- Flight dynamics and manoeuvre planning
- Telemetry analysis and telecommand generation
- Calculation of the starting and stopping time for the downlinks to be performed
- On-board software maintenance
- Mission simulation
- FOS supervision
- Interface with the launch site for LEOP

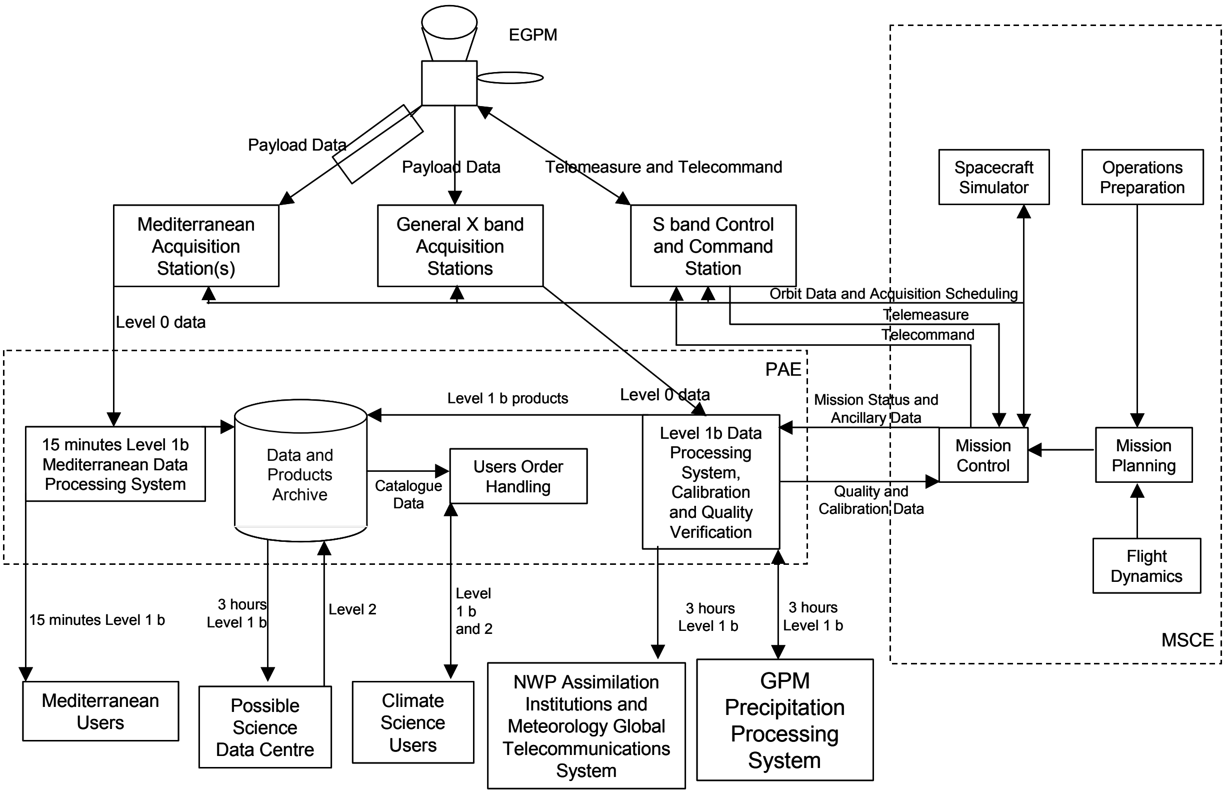

Figure 5.3: *Ground segment architecture*

The PAE will implement the following PDS functions:

- Acquisition of payload data (including platform ancillary data) from the CDAE
- Generation of products at level 1b by means of Instrument Processing (IPF) facilities
- Long-term archiving (LTA) of mission products, including re-processing of archived data as needed
- Payload Monitoring by means of a Monitoring Facility (MF). This includes calibration of the instruments
- Quality control (QC) for all products and media distributed to users.

- Distribution of level 1b products to the users
- Interfaces with the GPM PPS

The PPS of GPM receives Level 1b data from all contributing satellite missions and generates Level 1b and higher level products for distribution to the users community. EGPM Level 1b products shall be transmitted to the PPS as soon as processed. The EGPM ground segment will also receive the GPM data. The Mediterranean data will be processed to level 1b in Matera or at the PAE at ESRIN and put in a repository for fast access. All data will also be sent in parallel to the PAE for archiving.

6 Operations and Utilisation Concept

The amount of data generated by EGPM is relatively small, the satellite is rather conventional and the instruments are always on. Therefore, satellite operations are straightforward. During the operational phase, Kiruna will be used as the single S band station for uplinking of commands and downlinking of housekeeping telemetry. During LEOP Kiruna will be reinforced by additional ESA ground stations. One week is foreseen for the duration of the LEOP and four months for the commissioning. Standard operations will include:

- Continuous observations with both instruments including calibration in the observation sequence
- Uplink of commands
- Downlink of instruments data and of platform and instruments housekeeping telemetry
- Acquisition by ground stations, processing and forwarding of data to the MSCE/PAE
- Orbit determination based on the on-board GPS receiver, and calculation and scheduling of the downlink over Matera, Kiruna, Gatineau and Svalbard
- Weekly to monthly orbital corrections.

The satellite works autonomously and can operate up to 72 hours without ground contact. The satellite can remain in safe mode without ground intervention for weeks for all anticipated failures triggering the safe mode.

Concerning the utilisation concept, EGPM will be used as part of GPM; EGPM will provide access to GPM data and products.

7 Data Processing

This mission produces the following main data sets up to level 1:

Product Level	Title	Content
0	Raw data	Source data from both precipitation radar and microwave radiometer instruments consisting of time ordered, validated sequence of packets of instrument data. Packets of ancillary data containing attitude and orbit data and instrument status data are also included.
1a.11	MWR Uncorrected Channel Power	Internal to Level 1b processor, not generally available to users.
1a.12	Precipitation Radar Return Power	Return power measurement in each range cell without radiometric correction.
1b.11	MWR Calibrated Brightness Temperatures	Brightness temperature calibrated with cold and hot calibration sources. Each measurement is tagged with geolocation information.
1b.12	PR Calibrated Return Power	Conversion of count value of radar echoes to total received power and noise level into engineering value of dBm. Each measurement is tagged with geolocation information.

Table 7.1: *EGPM data levels*

The data processing is done in the PAE located in ESRIN. The data flow of the different levels of products can be seen in Figure 5.3. A fast processing chain will provide a parallel link for the delivery of the calibrated and geo-referenced 15 minute data. The 3 hours level 1 b data will be provided to GPM PPS and to meteorological institutions that will assimilate them in their operational Numerical Weather Prediction models.

8 Performance Aspects

8.1 Microwave Radiometer

The two concepts proposed for the microwave radiometer use slightly different technologies and thus have different performance figures. Since each concept has their advantages and drawbacks, a representative synthesis has been attempted here. In particular, at the high frequencies, lower radiometric noise would be achievable with the results of the ongoing bread-boarding activities. The values listed in Table 8.1 have been used in the performance assessment in Chapter 6 of the science report.

<table>
<tr><th>CENTRE FREQ. (GHZ)</th><th>Pol.</th><th>NEΔT (K)</th><th>abs. acc. (K)</th><th>IFOV (km×km)</th><th>Int. time (ms)</th><th>Along track sampl. interval (km)</th><th>Along track overlap factor (%)</th><th>Along scan sampl. interval (km)</th></tr>
<tr><td>18.7</td><td>H</td><td>0.36</td><td rowspan="2">0.44</td><td rowspan="2">25.4 x 14.9</td><td rowspan="3">13.2</td><td rowspan="9">13.4</td><td rowspan="2">47</td><td rowspan="3">26</td></tr>
<tr><td>18.7</td><td>V</td><td>0.39</td></tr>
<tr><td>23.8</td><td>V</td><td>0.28</td><td rowspan="3">0.4</td><td>24.8 x 15.0</td><td>46</td></tr>
<tr><td>36.5</td><td>H</td><td>0.38</td><td rowspan="2">13.6 x 8.0</td><td rowspan="6">6.8</td><td rowspan="2">1</td><td rowspan="6">13</td></tr>
<tr><td>36.5</td><td>V</td><td>0.38</td></tr>
<tr><td>50</td><td></td><td>0.39</td><td rowspan="4">0.43</td><td rowspan="4">12.1 x 6.6</td><td rowspan="4">-11</td></tr>
<tr><td>53</td><td></td><td>0.39</td></tr>
<tr><td>54</td><td></td><td>0.39</td></tr>
<tr><td>55</td><td></td><td>0.39</td></tr>
<tr><td>89</td><td>H</td><td>0.7</td><td rowspan="4">0.6</td><td rowspan="2">4.8 x 2.8</td><td rowspan="4">3.3</td><td rowspan="4">6.7</td><td rowspan="4">-34</td><td rowspan="4">6.5</td></tr>
<tr><td>89</td><td>V</td><td>0.7</td></tr>
<tr><td>89</td><td>H</td><td>0.7</td><td rowspan="2">5.2 x 3.0</td></tr>
<tr><td>89</td><td>V</td><td>0.7</td></tr>
<tr><td>118.75±1</td><td></td><td>0.9</td><td rowspan="4">0.66</td><td rowspan="4">13.0 x 7.0</td><td rowspan="4">6.8</td><td rowspan="4">13.4</td><td rowspan="4">-3</td><td rowspan="4">13</td></tr>
<tr><td>118.75±1.5</td><td></td><td>0.9</td></tr>
<tr><td>118.75±2</td><td></td><td>0.9</td></tr>
<tr><td>118.75±4</td><td></td><td>0.9</td></tr>
<tr><td>150</td><td>H</td><td>1.5</td><td rowspan="4">0.85</td><td rowspan="2">6.8 x 3.3</td><td rowspan="4">3.3</td><td rowspan="4">6.7</td><td rowspan="4">-10</td><td rowspan="4">6.5</td></tr>
<tr><td>150</td><td>V</td><td>1.5</td></tr>
<tr><td>150</td><td>H</td><td>1.5</td><td rowspan="2">5.4 x 3.2</td></tr>
<tr><td>150</td><td>V</td><td>1.5</td></tr>
</table>

Table 8.1: *Achieved radiometric and spatial performances of the EGPM radiometer channels. Pol.: Polarisation, NEΔT: Noise equivalent temperature sensitivity, IFOV: Instantaneous field of view*

The performance of the instrument has been simulated using standard modeling techniques. The radiometric noise produced by the different electronic components in the receiver chains as well as typical realistic atmospheric scenes have been used to simulate the radiometric measurements. Excluded from the modeling activities were the influence of the antenna patterns on the observations and the change of the natural atmospheric noise over the period during which all channels observed the same atmospheric scene. The results of the simulations are reflected in the column for the noise equivalent brightness temperature in Table 8.1.

With the exception of the noise at the highest frequency, the accuracy values are in line with the requirements of Table 4.1. Several along track overlap factors are negative, i.e. there are gaps in the coverage. Nevertheless, from the scientific point of view this is deemed acceptable. This simplifies the front-end accommodation problems in one of the two concepts. In the other concept, the number of channels in the 89 and 150 GHz bands is doubled This eliminates the gaps in these bands but results in a more elaborated design due to the need to accommodate the additional receivers.

Figure 8.1 shows the scan strategy to provide co-located observations of all channels within a period as brief as possible. This results from the arrangement of the feed horns as shown before in Figure 4.5. The scan direction is from the left of the figure to the right. In obtaining Figure 8.1, the proper allocations of pointing and alignment errors have been used and the footprints on the Earth surface have been derived. The nominal incidence angle of 52.8° is the centre of the footprint of most channels. The 52 and 119 GHz footprint are located two scans after the others. They will see the same point 4 seconds afterwards. The image acquisition of all channels can be considered simultaneous.

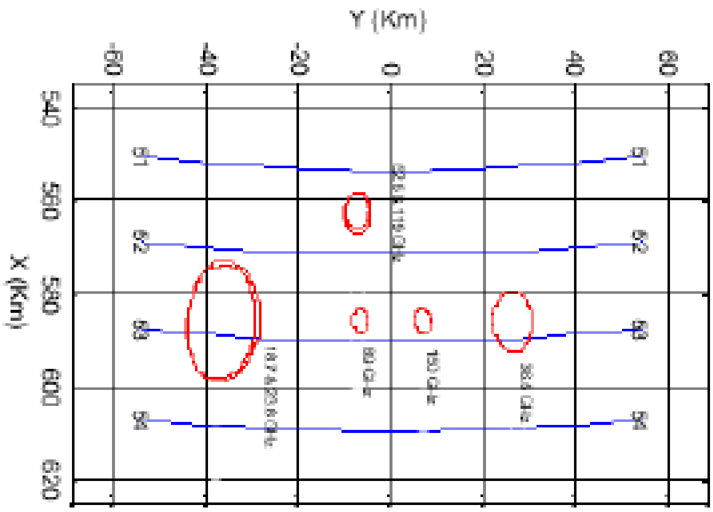

Figure 8.1: *Instantaneous field of view of the EGPM radiometer channels. The red lines are the footprints and the blue lines are the successive scan lines*

8.2 Performance Aspects of the Precipitation Radar

The radar performance has been estimated by simulation using the parameters listed in section 4.2.4. The results have been compared with the sensitivity and accuracy given in table 4.2. This is shown in figure 8.2 for the top of the precipitation layer. The radar echo is averaged on board to produce an along-track sampling interval of 1 km. As a minimum, the threshold requirements need to be met. The goal requirements are understood as "desirable".

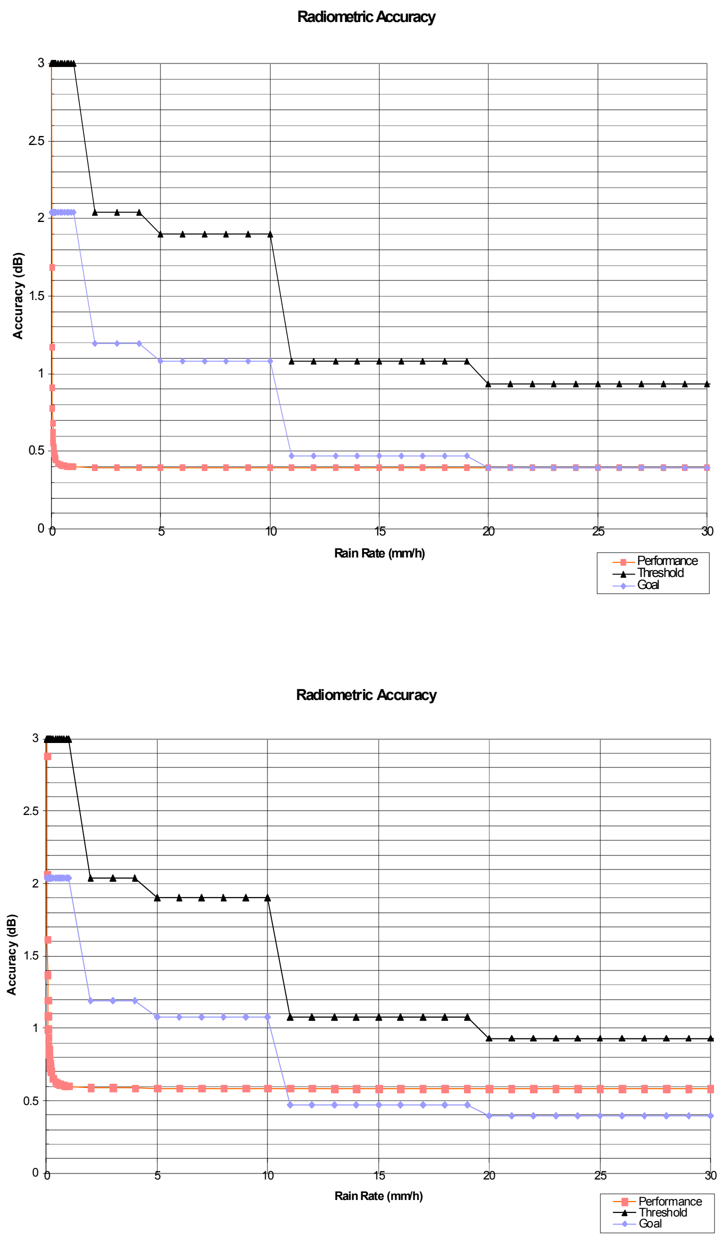

Figure 8.2: *Performance assessment showing the expected radiometric accuracies for an along-track integration distance of 4 km (top) and 1 km (bottom) at the top of the precipitation layer*

For the radar performance assessment, Z-R relationships have been used based on Marshall-Palmer distributions. The results in this section have to be interpreted as 'indicative' numbers.

Since the main objective for the radar is the detection of light rain and snow, the performance obtained for rates below 5 mm/h gives a good indication of the performance of the radar to meet the mission objectives. The initial assessments have been done assuming no attenuation (i.e. top of the layer), as for these rates the attenuation does not have a major influence.

For the rain case at the top of a precipitation layer, it can be seen from Figure 8.2 that with the present baseline configuration the threshold requirement (black line) is met with good margin for a 1 km along-track integration distance. The goal (blue line) is met with 4 km along-track integration. It is recalled that the accuracy requirements shown in Table 4.2 need to be fulfilled for an integration area (on-board plus on-ground) of less than 20 km × 20 km. For snow, the goal requirement is also easily met (not shown).

Similar analyses have been done for the bottom of the precipitation layer for different layer depths. The results are given in Table 8.3. The maximum precipitation rates are given per beam. For the 13 km × 13 km and 20 km × 13 km cases, averaged values for the 3 radar beams are also provided.

Layer depth	**1 km**		**2 km**		**3 km**		**4 km**		**5 km**	
ATID / *req*	*thresh*	*goal*	*thresh*	*goal*	*thresh*	*goal*	*thresh*	*goal*	*thresh*	*goal*
1 km	68	18	32	10	20.5	10	15.6	10	12.1	10
4 km	76.7	56	36.5	25.7	23.4	19.3	17	13.8	13.9	10.6
13 km	82.7	68	39.6	32	25.2	20.5	19	16.2	15.2	12.6
13 × 13 km^2	87.9	75	42.3	35.6	27.5	23	20.3	17.9	16.2	14
20 km	84.8	71	40.7	33.5	26.4	21.5	19.5	16.9	15.7	13.1
20 × 13 km^2	89.9	77.4	43.3	36.9	28.2	23.8	20.8	18.2	16.4	14.5

Table 8.3: *Maximum rain rates (mm/h) for different along-track integration distances (ATID) and layer depths to meet threshold and goal requirements*

A similar analysis has been made to derive the minimum radar sensitivity for different along-track integration distances. Since the threshold precipitation rate accuracy requirements for rain are the same as the goal requirements for snow, the values in the column $dBZ_{Threshold}$ (for rain) are also valid for the goal requirement for snow. Also here, the minimum radar sensitivity is indicated per beam, except for the 13 km × 13 km and 20 km × 13 km cases whereby all 3 radar beams have been used.

As can be seen from Table 8.4, a longer integration distance (the requirement is 20 km) will enhance the minimum radar sensitivity by roughly 7 dB.

Integration distance	**$dBZ_{Threshold}$**	**dBZ_{Goal}**
1 km	2.5 dBZ	5.1 dBZ
4 km	-0.7 dBZ	1.7 dBZ
13 km	-3.3 dBZ	-1.0 dBZ
13 × 13 km^2	-5.7 dBZ	-3.5 dBZ
20 km	-4.3 dBZ	-2.0 dBZ
20 × 13 km^2	-6.7 dBZ	-4.4 dBZ

Table 8.4: *Minimum radar sensitivity for different along-track integration distance to meet threshold and goal requirements*

9 Alternative Mission Concept

In addition to the baseline mission implementation described before, an alternative concept has been analysed though to lower level of detail. The payload is limited to the microwave radiometer. The rain radar is not embarked and the EGPM becomes a simple drone satellite. This reduces the complexity of the satellite. Its configuration will be identical to the baseline one but with the precipitation radar removed. The elimination of the radar will reduce mass by up to 85 kg and power needs by up to 55 W. It will also eliminate any problem related to the radio frequency compatibility between radar and radiometer. An optimization analysis of this descoped version has not been performed. Therefore the resulting snowball reduction effect has not been derived. One major drawback is that the radiometer cannot be calibrated with the radar for light rain and snow as the Ka-band radar of the "Core" GPM satellite has not enough sensitivity nor flies over latitude above 65°. At lower latitudes, the opportunities for coincidence of both missions are rare. In a period of 15 days, and considering 5 minutes as the limit to consider that both satellite observations are simultaneous, there are the following opportunities:

- For the GPM-Core flying at LTAN=22:30; 59 coincidences; 18 at latitudes below 20˚.
- For the GPM-Core flying at LTAN=06:30; 68 coincidences; 0 at latitudes below 20˚

10 Programmatic Aspects

The technical maturity of the EGPM mission was assessed during the first evaluation of the candidate Earth Explorer Opportunity Missions in 2002. Strong heritage was identified for the microwave radiometer based on Multifrequency Imaging Microwave Radiometer (MIMR), MADRAS for Megha-Tropiques, Microwave Humidity Sounder (MHS) of the EPS / Met***Op*** and the microwave radiometer of ENVISAT. Related technology developments, e.g. LNA, were also identified in the Agency's Technology Research Development Programme. Heritage was also identified for the precipitation radar from telecommunication systems and other radar missions. The development risks were associated with several well identified elements of the payload, namely: the scan mechanism of the microwave radiometer and the switching matrix of the precipitation radar (though the latter was based on the long-pulse solution).

During phase A additional areas requiring special attention have been identified. For the radiometer these result of the need for higher performance and more compact design, in particular for the high frequency channels. For the precipitation radar the areas of attention are the EIK /EPC and the ferrite switching network.

A summary of the maturity and development status of the critical technologies is reported in the table 10.1 below. These activities are still in progress or ready to be initiated.

Unit	Maturity and development status
Microwave Radiometer	
Scan Mechanism	This can built upon the experience of MIMR where a similar concept was developed. Recent developments on non contact transfer of power and signal shall be also taken into account.
Direct detection chain for the 89 GHz channel	Heterodyne detectors were qualified by MHS but a direct detection will allow reduction on mass, volume power consumption and sensitivity. Breadboard of LNA chip, filter and detector based on 70 µm metamorphic MMIC or OMMIC are being developed.
Filter at 54 GHz	A similar filter has already been developed in Madras but with lower quality. This development has been already started
Receiver chain for the 118 GHz channel	Conventional heterodyne architecture —as used in MHS— will not provide the required performance. The availability of a MMIC LNA using metamorphic process with high Indium contents will ensure the improvement of performances needed by the mission.
Dual frequency feed-horn for 54 / 118 GHz	Needed to allow better accommodation of the feed-horns. Development initiated.
Precipitation Radar	
Radar EIK	Action initiated during phase A by the Canadian Space Agency. This development can use as starting point the EIK developed for the Cloudsat and the ESA Explorer EarthCARE missions
Ferrite switches	On-going early development activity initiated within phase A

Table 10.1: *Maturity of instrument technologies and development status*

According to the results of the phase A industrial teams, the EGPM implementation is driven by the development of the payload. Concerning the microwave radiometer, breadboards are recommended to be completed for the receivers and for the scan mechanism. For the rain radar no new technology is required but adaptation of existing technology is needed. This will require also several breadboards / engineering models.

No critical elements have been identified for the platform development since there is a strong heritage from on-going Earth Explorers and other Low Earth Orbit (LEO) missions.

At satellite level, a proto-flight model (PFM) approach is baselined by the phase A system contractors. An avionics test bench (model based development environment) is proposed for validation of the compatibility of the avionics and AOCS elements, including interfaces with the payload, using the breadboards and engineering models mentioned above.

An area of risk is the verification of the radio frequency compatibility between radar and radiometer. Complementary approaches have been identified:

- Specific analysis, but the level of credibility of an analysis-only approach is limited
- Early mock-up testing, but the validity is limited by the representativity of the mock-up with respect to the final satellite configuration
- Comprehensive test on the PFM of the satellite. This test will be very late in the EGPM programme.

The approach to the interference problem will be defined after supplementary analysis in the next phase of the programme.

The ground segment development is based on existing infrastructure. For product development the experience with TRMM will be very valuable.

With the exception of the radiometer scan mechanism, none of the developments above is considered schedule critical. The development schedule proposed in phase A can be seen in table 10.2. It could lead to launch in 2009 / 2010.

Development Phase	Duration in months
Pre-development and Phase B	12 - 18
Phase C/D	45 - 48

Table 10.2: *Development schedule*

11 References

Phase A System Study for the EGPM mission (EADS Astrium) Final Report March 2004. Contract 17213/03/NL/GS

Phase A System Study for the EGPM mission (CGS) Final Report. March 2004. Contract 17214/03/NL/GS